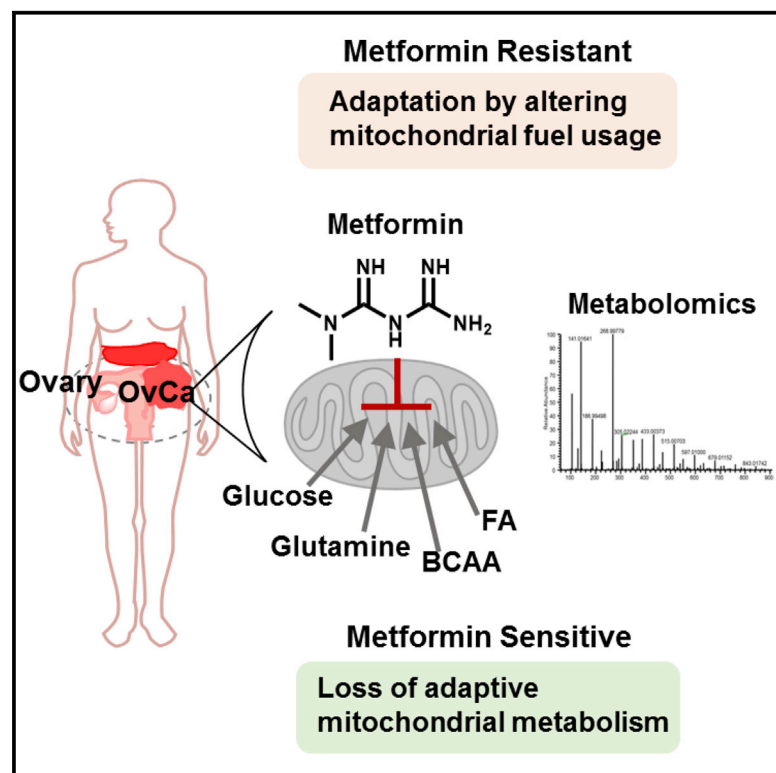# Metformin Targets Central Carbon Metabolism and Reveals Mitochondrial Requirements in Human Cancers

Graphical Abstract

Authors

Xiaojing Liu, Iris L. Romero, Lacey M. Litchfield, Ernst Lengyel, Jason W. Locasale

Correspondence

jason.locasale@duke.edu

In Brief

Liu et al. carry out an integrative metabolomics analysis of metformin action in ovarian cancer. Using patient samples (including those from a "super-responder"), animal tumors, and cell culture models, they find that the predominant mechanism of action by metformin in cancer is to target tumor-cell-intrinsic mitochondrial metabolism.

Highlights

- Metformin accumulates in human tumor biopsies at micromolar concentrations

- The response to metformin in humans can be modeled in nutrient-limited environments

- Mitochondrial substrate utilization underlies metformin sensitivity

- Restoration of specific mitochondrial outputs causes resistance to metformin

CrossMark

CellPress

Metformin Targets Central Carbon Metabolism and Reveals Mitochondrial Requirements in Human Cancers

Xiaojing Liu,[1] Iris L. Romero,[2] Lacey M. Litchfield,[2] Ernst Lengyel,[2] and Jason W. Locasale[1,3,*]

[1]Department of Pharmacology and Cancer Biology, Duke Cancer Institute, Duke Molecular Physiology Institute, Duke University School of Medicine, Durham, NC 27710, USA
[2]Section of Gynecologic Oncology, Department of Obstetrics and Gynecology, Center for Integrative Science, University of Chicago, Chicago, IL 60637, USA
[3]Lead Contact
*Correspondence: jason.locasale@duke.edu
http://dx.doi.org/10.1016/j.cmet.2016.09.005

SUMMARY

Repurposing metformin for cancer therapy is attractive due to its safety profile, epidemiological evidence, and encouraging data from human clinical trials. Although it is known to systemically affect glucose metabolism in liver, muscle, gut, and other tissues, the molecular determinants that predict a patient response in cancer remain unknown. Here, we carry out an integrative metabolomics analysis of metformin action in ovarian cancer. Metformin accumulated in patient biopsies, and pathways involving nucleotide metabolism, redox, and energy status, all related to mitochondrial metabolism, were affected in treated tumors. Strikingly, a metabolic signature obtained from a patient with an exceptional clinical outcome mirrored that of a responsive animal tumor. Mechanistically, we demonstrate with stable isotope tracing that these metabolic signatures are due to an inability to adapt nutrient utilization in the mitochondria. This analysis provides new insights into mitochondrial metabolism and may lead to more precise indications of metformin in cancer.

INTRODUCTION

Metformin, a biguanide, is a commonly prescribed agent for the management of type II diabetes. It is widely used clinically because of its desirable safety profile and reproducible actions on systemic glucose homeostasis, which lead to the reduction of glucose levels during hyperglycemia (Knowler et al., 2002). Its effects are attributed to suppression of hepatic gluconeogenesis, reduction of glucose absorption in the intestine, alterations in the composition of the gut microbiota, and direct control of glucose metabolism in muscle, subcutaneous, and visceral adipose tissue (Forslund et al., 2015; Fullerton et al., 2013; Madiraju et al., 2014; Zhou et al., 2001). The precise mechanism of action in diabetes, however, remains controversial (Pernicova and Kor-

bonits, 2014). In epidemiological studies, metformin has been associated with reduced incidence in cancers such as breast, prostate, colorectal, endometrial, and ovarian (Decensi et al., 2010; Evans et al., 2005; Jiralerspong et al., 2009; Romero et al., 2012). Furthermore, a prospective clinical trial in non-diabetic patients showed its efficacy in patients presenting with adenomatous polyps when administered after surgical resection (Higurashi et al., 2016). Moreover, multiple clinical trials using metformin as a treatment in non-diabetic cancer patients are ongoing (Camacho et al., 2015).Thus, there is significant interest in using metformin as a cancer therapeutic, especially in cancers with limited treatment options, such as ovarian cancer (OvCa) (Bowtell et al., 2015; Febbraro et al., 2014). The mechanism of its anti-cancer properties has also been controversial, and it remains poorly understood whether metformin acts by altering host metabolism or by direct action on tumor cells (Chandel et al., 2016; Dowling et al., 2016). Further clinical advances are limited by controversies surrounding the biology of metformin and the poorly understood determinants of a response that lead to biomarkers that can be used to predict which patients may benefit.

At the cellular level, metformin is believed to disrupt mitochondrial function by partially inhibiting nicotinamide adenine dinucleotide (reduced form) (NADH) dehydrogenase (Wheaton et al., 2014) in general or by inhibiting glycerol phosphate dehydrogenase in liver cells, which also results in alterations to the electron transport chain (ETC) (Madiraju et al., 2014). As a result, electrons contained in NADH and flavin adenine dinucleotide (reduced form) ($FADH_2$) are not as effectively transported through the ETC. Because each of these processes is central to numerous aspects of cell physiology, the cellular effects of metformin are pleiotropic. For example, it has been documented to affect AMPK signaling, protein kinase A signaling, folate metabolism, and anabolic metabolism (Birsoy et al., 2014; Cabreiro et al., 2013; Griss et al., 2015; Janzer et al., 2014; Madiraju et al., 2014; Miller et al., 2013; Shaw et al., 2005; Wheaton et al., 2014; Zhou et al., 2001). Most of these mechanisms point to mitochondrial biology as its mechanistic target.

Mitochondria utilize glucose, amino acids, and fatty acids as substrates to allow for ATP production, redox balance, and biomass precursor production. Thus, metformin results in alterations to the tricarboxylic acid (TCA) cycle, the generation of
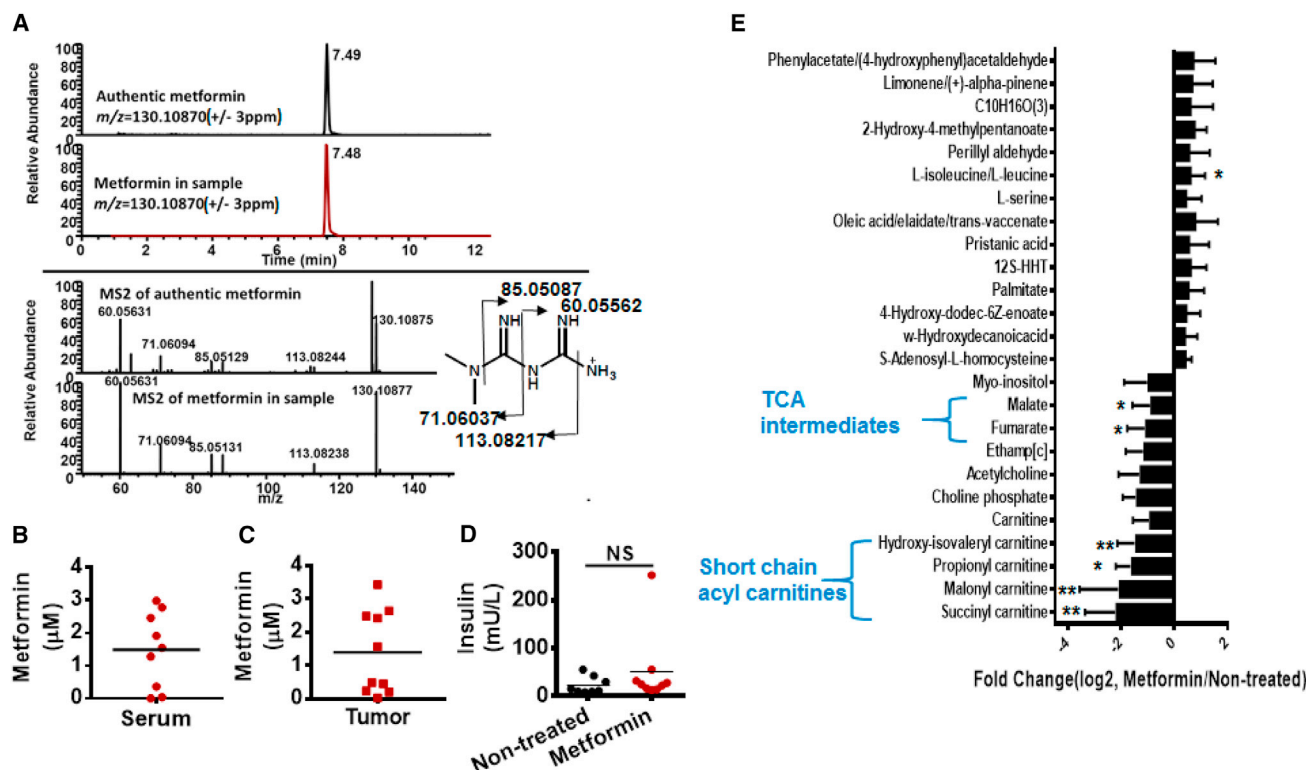
Figure 1. Altered Mitochondrial Metabolism in Human Ovarian Tumors from Patients Taking Metformin

(A) Extracted ion chromatogram of an authentic standard of metformin (top) and of metformin extracted from mouse serum (bottom) with an *m/z* window of 6 ppm (± 3 ppm). MS2 spectrum of authentic metformin (top) and metformin extracted from mouse serum (bottom).

(B) Metformin levels in serum of ovarian cancer (OvCa) patients.

(C) Metformin concentration in ovarian tumors from patients.

(D) Insulin levels in the serum of OvCa patients after overnight fasting.

(E) Metabolites with trending changes (p < 0.1, *p < 0.05, **p < 0.01, two-tailed Student's t test) in tumors from patients on metformin compared to tumors not exposed to metformin treatment (n = 10). The fold change is calculated by dividing MS intensity (integrated peak area of metabolites) values of each metabolite in metformin treated patient tumors by those with no metformin treatment. Error bars obtained from SEM of n = 10 measurements from individual patients.

reactive oxygen species, alterations of the mitochondrial phosphate to oxygen ratio that affects ATP production, and other essential mitochondrial functions. For example, it has recently been reported that one such essential function is to provide aspartate, which is used for the synthesis of nucleotides and protein (Birsoy et al., 2015; Cardaci et al., 2015; Sullivan et al., 2015). Other studies have found that metformin alters lipid synthesis from the mitochondria by affecting reductive carboxylation (Fendt et al., 2013). Consistently, metformin has also been found to suppress nucleotide levels (Janzer et al., 2014). Each of these mechanisms occurs through changes in the capacity of the ETC.

In light of this extensive body of literature, there is a lack of analysis of metabolism in physiological environments, where clinically relevant metabolic signatures of metformin-associated cytotoxicity can be observed. This limits many of these findings, and it is thus not understood how mitochondrial metabolism is altered to produce these changes and what compensatory pathways induced by disruption of the ETC must be overcome for metformin-induced cytotoxicity. There is, furthermore, a lack of direct study of metformin action on tumor metabolism in patients and comparisons to mechanisms observed in cell culture and in

animal models. With the advent of recent metabolomics approaches, multiple aspects of tumor cell metabolism can be profiled in patient samples (Liu et al., 2014). We therefore hypothesized that such experiments could shed light on the anti-cancer mechanisms of metformin when integrated with studies on experimental models.

RESULTS

Altered Mitochondrial Metabolism in Human Tumors from Patients Taking Metformin

There has been a paucity of data surrounding the concentration of metformin that can be achieved in human tumors. We first developed a sensitive and quantitative method using liquid chromatography coupled to high-resolution mass spectrometry (LC-HRMS) to quantify metformin concentrations in tissue and serum. With an authentic reference compound and fragmentation pattern from tandem mass spectrometry (Figure 1A), we were able to unequivocally identify and quantify metformin in the sera (Figure 1B) and tumors (Figure 1C) of patients taking metformin prior to surgery and found concentrations reaching micromolar values. Interestingly, no differences in the insulin

levels in these patients were observed (Figure 1D). We then generated a metabolite profile (Liu et al., 2014) of the tumors from ten patients taking metformin presenting with stage III and/or IV high grade papillary serous OvCa (Figure S1A, available online) compared to ten patients not taking metformin with similar diagnoses, ages, and medication profiles. An inspection of the profile (Figure 1E) showed that most of the more than 300 metabolites measured did not show a difference indicating extensive heterogeneity as expected (Hensley et al., 2016). Interestingly, TCA intermediates and short chain acyl carnitines (succinyl carnitine and branched chain acyl carnitines), both related to mitochondrial metabolism (Koves et al., 2008; Liu et al., 2015), were the classes of compounds most frequently suppressed in the tumors of metformin-treated patients. Three of the known functions of mitochondrial metabolism are to maintain nucleotide levels, energy status, and oxidation status (Shadel and Horvath, 2015; Weinberg and Chandel, 2015; Zong et al., 2016). In each case, and as is expected since cancer is a heterogeneous disease, there was large variation in metabolites involved in each of these processes, with some patients exhibiting alterations in the metabolites involved in each of these functions (Figures 1E and S1B–S1D). Long chain acyl carnitines, markers of fatty acid oxidation (Koves et al., 2008), were variable in the patient tumors, indicating that a defect in fatty acid oxidation, although possibly present in certain tumors, was not commonly observed (Figure S1E). Together, these results indicate that metformin accumulates in human tumors and affects known mitochondrial biology.

Therapeutic Doses of Metformin Directly Suppress Tumor Mitochondrial Metabolism

The metabolomics of human tumors (Figure 1) appear consistent with the conclusion that metformin affects cell intrinsic mitochondrial metabolism. Nevertheless, these studies involved a limited set of patient samples. We therefore considered laboratory models of ovarian cancer. HeyA8 cells were injected in the intraperitoneal cavity of female mice and tumors formed in the omentum, resembling a serous-papillary cystadenocarcinoma (Lengyel et al., 2014) (Figure 2A). Treatment of mice 2 weeks after initiation of OvCa showed that metformin effectively reduced tumor weight (p = 0.01, one-tailed Student's t test) (Figure 2B) and the concentration of metformin reached micromolar concentrations in serum (Figure 2C) and tumor (Figure 2D). Both serum and intratumoral levels of metformin correlated (p = 0.07, p = 0.03, respectively, Spearman's correlation coefficient) with treatment response. As observed in the patients, insulin levels in mouse serum were unaffected (Figure 2E). Metabolite profiles from metformin- and vehicle-treated animal tumors were generated using LC-HRMS (Figure 2F) and first analyzed by a principle component (PC) analysis (Figure 2G), revealing that the largest source variation in the cohort was treatment. Metabolites enriched in the pyrimidine and/or purine metabolism pathways and the glutathione pathway (Figure 2H) contributed to the first PC. Metabolites involved in nucleotide synthesis (Figure 2I), redox status indicated by increased oxidized glutathione (GSSG) levels (Figure 2J), and energy status (Figure 2K) were generally reduced. Together, these findings indicate that metformin affects several features related to mitochondrial metabolism in animal tumors.

A Metformin-Treated Patient with an Exceptional Outcome Shares the Metabolic Profile of the Animal Tumors Responding to Metformin

While the metabolic profile of the metformin response in human tumors was variable, metformin treatment in controlled settings using laboratory animals appeared reproducible. Of note, the time to recurrence was also variable in the patients taking metformin, and one patient exhibited an exceptionally long disease-free interval (long-term survivor) with no recurrence to date (Figure 3A). Although single patient responses have long been considered merely anecdotal in nature and lacking statistical rigor, there have recently been considerable advances made by using these observations to understand the mechanism underlying these exceptional outcomes (Grisham et al., 2015; Marx, 2015; Wagle et al., 2014). Utilizing this long-term survivor, we sought to compare the metabolic features of this patient, the cohort of patients, and the mouse responding to metformin. Overall, a small amount of overlap in the profiles of the animal tumors and the patients was observed. Remarkably, when comparing this long-term survivor, a substantial amount of the metabolome overlapped with the signature in the mouse ovarian tumor responding to metformin (Figure 3B). An analysis of overlapping features (Figure 3C) revealed decreases in acyl-carnitines, nucleotides, and glutathione-related metabolites and increases in nucleotide intermediates, suggesting a buildup in these pathways. These intriguing results indicate a possible cell-intrinsic human signature of a response to metformin in ovarian cancer.

In Vivo Metabolite Profiles of Metformin Response Can Be Modeled in a Glucose-Limited Environment

We next questioned the specific biochemical events and environmental conditions that directly give rise to these correlative signatures seen in human and mouse xenograft tumors. Although serum levels of glucose in the mice and humans were in the range of 5–10 mM (Figure 4A), the values measured in human and mouse tumors were markedly lower, ranging from 0–1 mM (Figure 4B). We thus reasoned that the metformin responses observed in vivo may require limiting mitochondrial substrate availability in the glucose-deprived tumor microenvironment. To test this hypothesis, we generated a metabolite profile in HeyA8 cells treated with metformin or vehicle in glucose-limited (1 mM) conditions that mimic the tumor microenvironment (Figure 4C). Notably, intracellular metformin concentration could reach values comparable to that of the culture media (Figure 2C). An increase in NADH, indicating disruption of ETC (Figure S2B), was observed with no changes in glucose uptake and lactate secretion fluxes (Figures S2C and S2D). Moreover, decreases in glutathione-related metabolites were also observed (Figure 4C) in addition to depletions in the TCA cycle (Figure 4D) and nucleotide levels (Figure 4E). An additional feature associated with ETC inhibition, involving a decrease in short chain acyl carnitines metabolites, was observed (Figure S2E), which was consistent with observations in patient (Figure 1E) and mouse tumors (Figure S2F). Notably, metformin also induced an increase of NADH in glucose-rich medium (Figure S2G), indicating metformin also targets on the ETC when there is sufficient glucose. However, no changes in glutathione (GSH)-related metabolites (Figure S2F), TCA intermediates
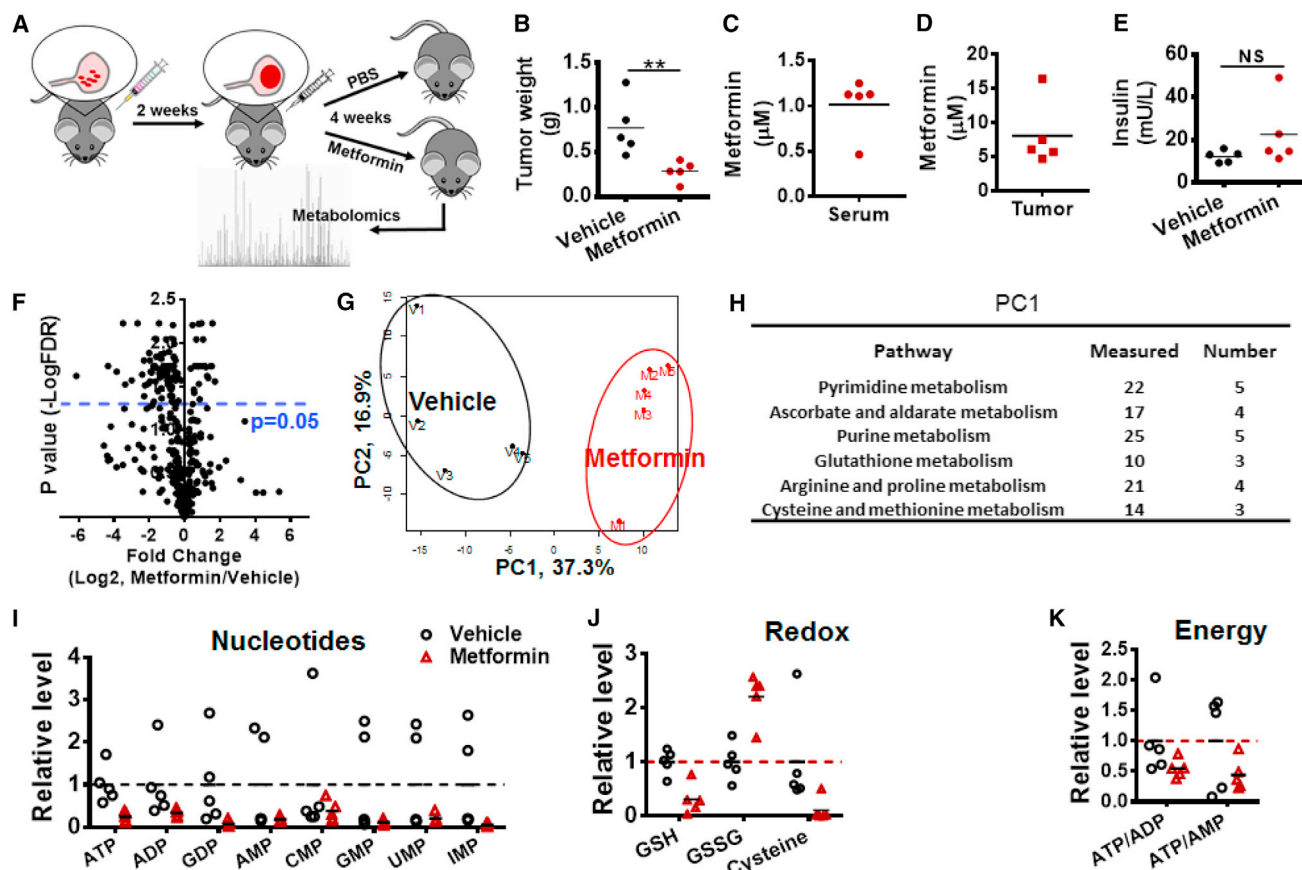
Figure 2. Metformin Directly Suppresses Tumor Mitochondrial Metabolism in Mouse Ovarian Tumors

(A) Description of timeline and treatment of the ovarian cancer model where HeyA8 cells are injected intraperitoneally.

(B) Mouse tumor weight (n = 5).

(C) Metformin concentration in mouse serum.

(D) Metformin concentration in mouse tumor.

(E) Insulin levels in mouse serum.

(F) Volcano plot of metabolites in mouse tumor.

(G) PCA analysis of metabolites in mouse tumor.

(H) Pathway analysis of metabolites in mouse tumor. "Measured" is the total number of metabolites detected in mouse tumor, and "Number" is the number of metabolites with significant changes (p < 0.05) in the metformin treatment group.

(I–K) Metabolites related to nucleotides (I), redox (J), and energy state (K). *p < 0.05, **p < 0.01.

(Figure S2H), or nucleotides were observed (Figure S2I), indicating that global metabolic reprogramming is not induced upon metformin treatment in high glucose conditions. Thus, most of the metabolic alterations found in metformin-responsive mouse and human tumor tissues can be reproduced in glucose-limited conditions, but not in high-glucose conditions, observed in typical cell culture media.

Metabolite Profiles of Metformin Are the Result of Altered Substrate Utilization in the Mitochondria

Although metabolite levels are direct reflections of physiological status, their interpretation is confounded by the dynamic nature of metabolism that involves the flow of nutrients or flux (Zamboni et al., 2015). Therefore, the utilization of each key macronutrient that is catabolized in the mitochondria was investigated. Stable isotopes of carbohydrate (U-^{13}C glucose), lipid (U-^{13}C palmi-

tate), and amino acid (U-^{13}C glutamine) were used to trace the fate of mitochondrial substrate utilization in response to metformin treatment (Figure 5A). Glucose entry into the mitochondria, as measured by the mass isotopologue patterns of citrate (Figure 5B), glutamine (Figure 5C), and palmitate (Figure 5D) in the TCA cycle were each affected by metformin treatment. In addition glucose-derived (Figure 5E), glutamine-derived (Figure 5F), and palmitate-derived (Figure 5G) aspartate, an intermediate for pyrimidine synthesis, were decreased, as were corresponding labeling patterns of glucose-derived (Figure 5H) and glutamine-derived (Figure 5I) pyrimidine that originate from the TCA cycle. Moreover, glutathione biosynthesis, which uses glutamate generated from the TCA cycle, was reduced (Figures S3A–S3D). However, addition of the antioxidant N-acetylcysteine (NAC) didn't increase GSH levels in the absence of metformin (Figure S3E), but it decreased glutathione disulfide (GSSG) levels
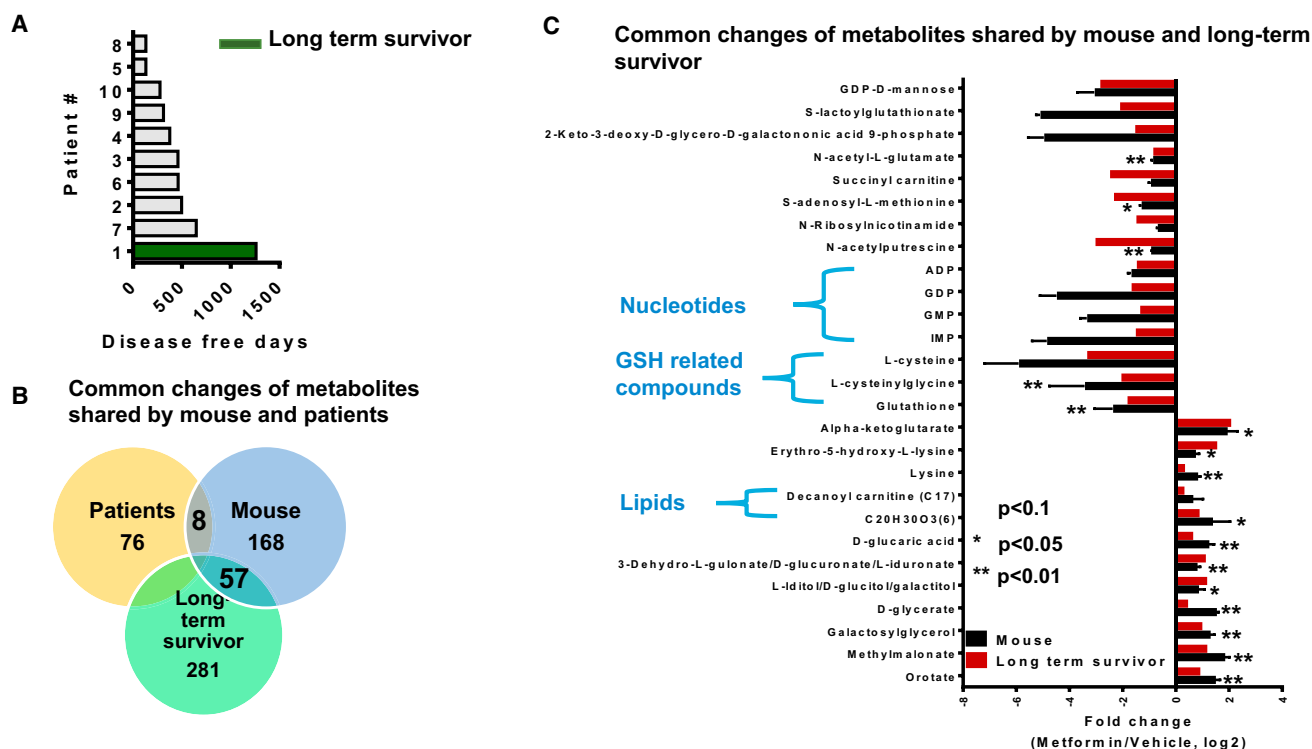
Figure 3. Metabolite Changes Are Shared by Patient and Mouse in Response to Metformin Treatment
(A) Disease-free days of ten patients on metformin. The long-term survivor patient is the one with the longest disease-free days (shown in green).
(B) Number of metabolites overlapped in patients and mouse tumor with larger effects in the metformin treatment group (fold change > 2 or < 0.6). This number indicates the number of metabolites with changes in response to metformin treatment.
(C) Representative metabolites sharing similar changes in response to metformin treatment in mouse ($p < 0.1$, *$p < 0.05$, **$p < 0.01$) and long-term survivor patient tumor. Error bars obtained from SEM of $n = 5$ mice.

(Figure S3F). Surprisingly, intracellular aspartate levels remained constant in the presence of metformin (Figure S4A), and, meanwhile, aspartate was actively exported out of the cell, indicating its excess rather than limitation (Figure S4B). Indeed, compared to cells grown in high glucose, there was also a decreased uptake of non-essential amino acids, such as lysine and leucine and/or isoleucine (Figures S4C and S4D), which further demonstrates the decreased consumption of these amino acids in low glucose environments. Together, these findings suggest that metformin alters substrate utilization and anabolic metabolism in the mitochondria, with anabolic metabolism being affected by a previously uncharacterized aspartate overflow mechanism.

Metformin Response and Resistance Are Determined by the Availability of Specific Nutrients
Next, we asked whether the nutrients utilized and metabolic outputs generated by mitochondria determine the cytotoxic effects of metformin. Consistent with previous observations (Birsoy et al., 2014; Litchfield et al., 2015; Wheaton et al., 2014), we found that HeyA8 OvCa cells are resistant to metformin in nutrient-rich conditions containing typical concentrations of glucose in culture media. When subjected to nutrient-limiting conditions, including glucose and amino acid deprivation, these cells become sensitive to metformin, implying that these environments impose sensitivity to metformin (Figure 6A). Annexin V and propidium iodide staining of HeyA8 cells in glucose-limited

(vehicle) and glucose-complete media (+glucose) demonstrated that glucose availability affects metformin-induced apoptosis and cell death in this model (Figure 6B). Furthermore, oxidative stress involving sub-lethal concentrations (30 μM) of hydrogen peroxide (Figure 6C) sensitized cells to metformin-induced cell death. Interestingly, the tumor from the long-term survivor (Figure 6D) exhibited low levels of glucose and a higher oxidative state as measured by glutathione potential and other related metabolites. Similarly, increased oxidative stress was also observed in metformin-treated cells (Figure 6E). To understand the metabolic features that underlie this sensitivity, we attempted to rescue metformin cytotoxicity using a series of nutrients. Cell number was quantified using both a colorimetric tetrazolium-based assay and direct cell counting. We found that pyruvate, an esterified version of α-ketoglutarate (DMKG), acetate, and α-ketobutyrate (Sullivan et al., 2015), all immediate mitochondrial substrates, were able to rescue metformin-induced cytotoxicity to various degrees (Figure 6F). Furthermore, we investigated downstream pathways altered by metformin and observed that nucleosides, deoxynucleotide triphosphates (dNTPs) (Figure 6G), or N-acetyl cysteine (NAC) (Figure 6H) exhibited modest but significant effects on rescuing cytotoxicity. The combinations of NAC with nucleotides, nucleosides, acetate, or α-ketobutyrate could, to a larger extent, rescue cells from metformin-induced cell death (Figure 6I). Importantly, results from the tetrazolium colorimetric assay were consistent
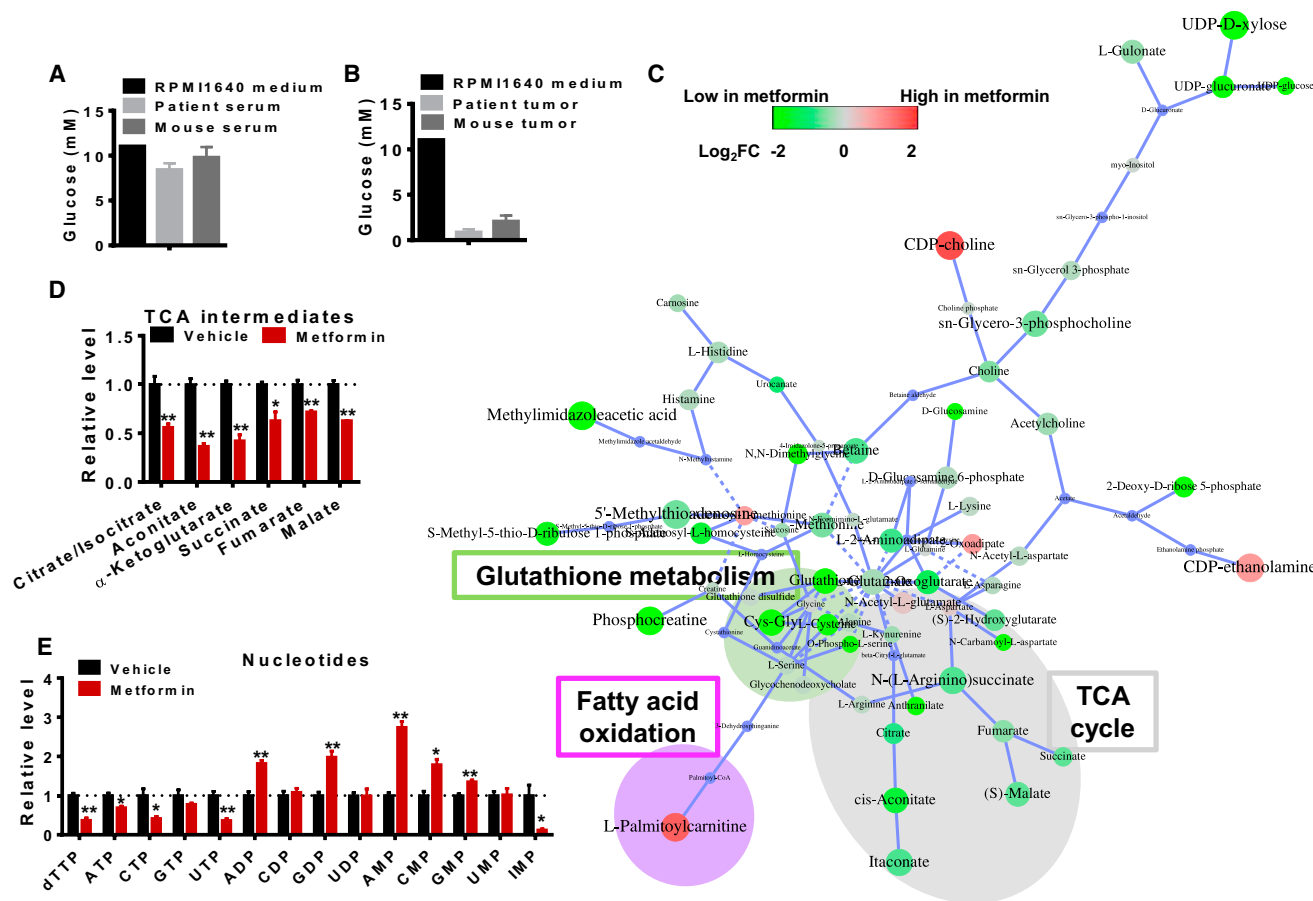
Figure 4. In Vivo Metabolite Profiles of Metformin Treatment Can Be Modeled in a Glucose-Limited Environment

(A) Glucose concentrations in RPMI medium, patient, and mouse serum.

(B) Glucose concentration in RPMI medium, patient, and mouse ovarian tumors.

(C) Network of significant metabolic changes in ovarian cancer cells in response to metformin treatment. The node size represents the p value, and the color represents the fold change. The size of the node indicates the magnitude of the change. Red represents metabolites that are higher in metformin-treated cells, and green denotes metabolites that are lower in metformin-treated cells.

(D and E) Representative metabolites among TCA (D) and nucleotides (E). The relative level was calculated by dividing MS intensity of each metabolite by corresponding MS intensity in the vehicle. *p < 0.05, **p < 0.01. Error bars obtained from SEM of n = 3 independent measurements.

with those obtained both from cell counting and cell imaging (Figures S5A–S5E). The supply of aspartate has been proposed to be an essential role of the electron transfer chain (Birsoy et al., 2015; Cardaci et al., 2015; Sullivan et al., 2015), but aspartate alone failed to rescue metformin-induced cell death, while the combination with NAC exerted only a modest effect (Figure S5F). Taken together, these results demonstrate that, consistent with signatures of metformin response in mice and humans, metformin cytotoxicity is caused by limited mitochondrial substrate availability and that redox and nucleotide biosynthesis are the critical functions required for cell viability in the presence of metformin. In agreement, redox status was preserved with the addition of mitochondrial substrates or NAC (Figure 6J) and oxidative stress was diminished (Figure 6K). Furthermore, we found that metformin also decreased energy status (ATP/ADP and ATP/AMP), and this effect was partially recovered in all four conditions that rescued cell proliferation (Figure S6A). Increased NADH/nicotinamide adenine dinucleotide (oxidized form) (NAD^+) due to NADH accumulation, however, was not rescued by these nu-

trients (Figure S6B). This finding is in contrast to previous observations, where pyruvate preserved the NAD^+/NADH ratio in the presence of electron chain transport inhibitors (Sullivan et al., 2015). The discrepancy highlights the heterogeneity of metabolic requirements and likely depends on other fluxes that metabolize NAD^+. TCA intermediates were dramatically elevated by pyruvate acid (PYR) and DMKG, but not by NAC or nucleosides (Figure S6C). Similarly, nucleotide levels are also differentially regulated by these nutrients (Figure S6D). Therefore, these findings additionally confirm that redox, energy homeostasis, and nucleotide biosynthesis in combination appear to be determining factors to the cytotoxic response in these environments.

The Response to Metformin Depends on whether Substrate Utilization in the Mitochondria Is Flexible

Altered nutrient utilization in cells with defective mitochondria is well documented with numerous pathway fluxes involved (Fendt et al., 2013; Worth et al., 2014). These include pyruvate carboxylase, reductive glutaminolysis, and branched-chain amino acid
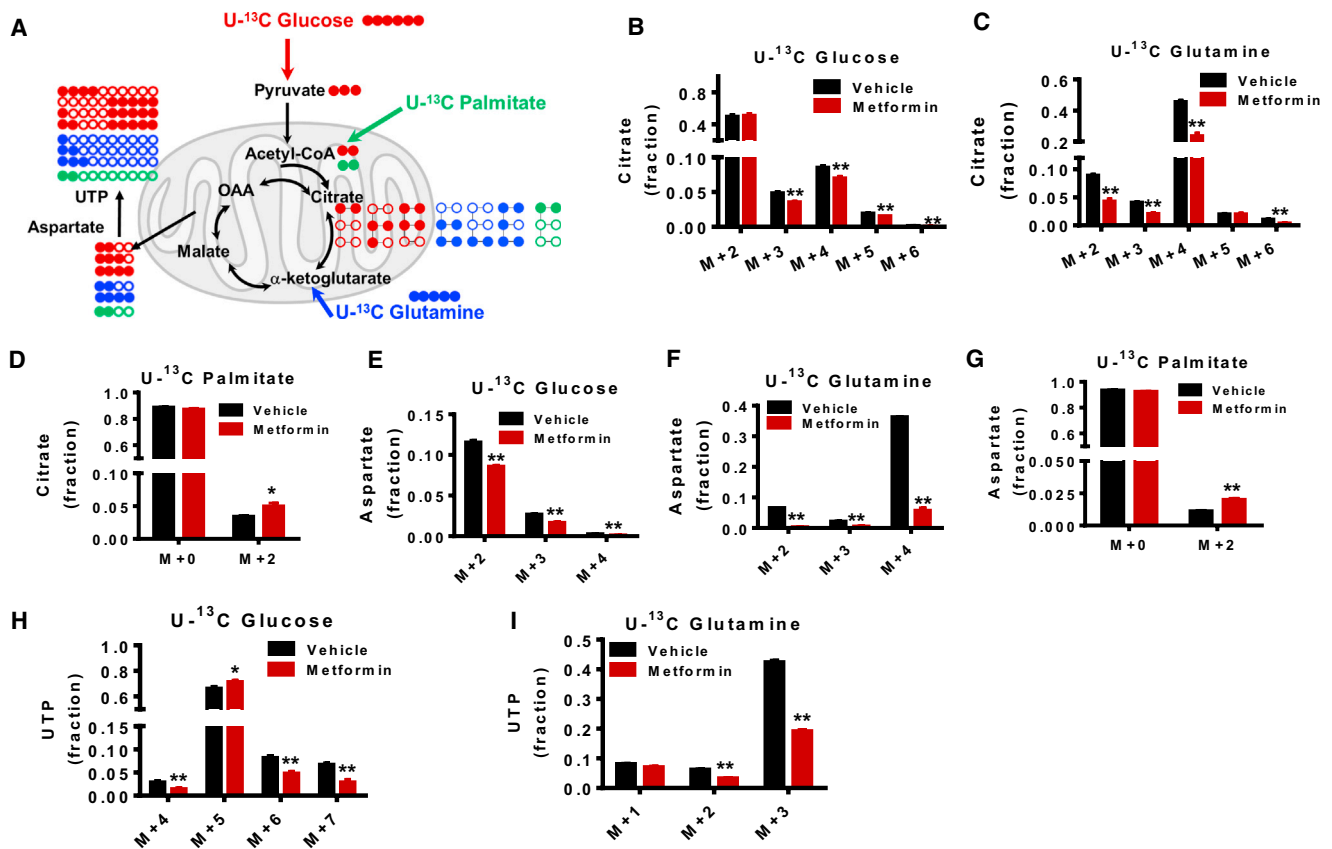
Figure 5. Metabolite Profiles of Metformin Are the Result of Altered Substrate Utilization in the Mitochondria

(A) ^{13}C enrichment patterns that are derived from different ^{13}C-labeled fuel sources. The solid circle denotes ^{13}C carbon, and the open circle denotes ^{12}C carbon.

(B–D) ^{13}C isotopologues' distribution of citrate from cells treated with ^{13}C-labeled glucose (B), glutamine (C), or palmitate (D) for 6 hr.

(E–G) ^{13}C enrichment in aspartate from ^{13}C-labeled glucose (E), glutamine (F), or palmitate (G).

(H and I) UTP ^{13}C distribution in the presence of ^{13}C-labeled glucose (H) or glutamine (I). ^{13}C-labeled UTP was not detected from ^{13}C-labeled palmitate. *p < 0.05, **p < 0.01. Error bars obtained from SEM of n = 3 independent measurements.

oxidation (BCAA), which are used as compensatory pathways when cells with functioning mitochondria are under mitochondrial stress (Figure 7A). In glucose-limited conditions, cells were unable to increase reductive glutaminolysis activity when oxidative glutamine metabolism was inhibited by metformin, while the presence of PYR, DMKG, NAC, or glucose caused up-regulation of the activity of this pathway upon treatment with metformin (Figure 7B). Moreover, the addition of excess glucose (11.1 mM) increased pyruvate carboxylase activity in response to metformin and maintained a stable carbon supply in the mitochondria (Figure 7C). In contrast, when glucose-limited, these cells were not able to use this pathway. Moreover, branched-chain amino acid oxidation (BCAA), also a pathway used as a fuel source, was significantly diminished by metformin treatment and recovered with addition of PYR, DMKG, or glucose (Figure 7D). Consistently, pyruvate was found to increase the concentration of TCA cycle intermediates (Figure S6C). Indeed, upon adding U-^{13}C pyruvate for 6 hr, citrate (M+2) and malate (M+3), representing flux into the TCA cycle through citrate synthase and pyruvate carboxylase, were both increased (Figure 7E), as was alanine (M+3), indicating transamination and generation of α-ketoglutarate (Figure 7F). Thus, the inability to

use these adaptive pathways in the TCA cycle in response to metformin treatment contributes to the sensitivity in glucose-limited conditions (Figure 7G).

DISCUSSION

Cell-Intrinsic Metabolic Reprogramming by Metformin in Tumors

Epidemiological data have strongly associated metformin usage with improved cancer outcomes in multiple cohorts in numerous different cancers, including OvCa (Decensi et al., 2010; Evans et al., 2005; Ezewuiro et al., 2016; Jiralerspong et al., 2009; Libby et al., 2009; Romero et al., 2012; Wright and Stanford, 2009). However, understanding how metformin might act to protect against or treat cancer has been complicated by controversies concerning its mechanism of action and the organ site on which it acts. By quantifying metformin concentrations in patient and mouse tumors, we were able to show it accumulates in tumors at concentrations that are sufficient to induce metabolic alterations consistent with changes in the activity of the electron transport chain. Importantly, the extent of the anti-tumor effect correlated with the amount of the compound that was measured
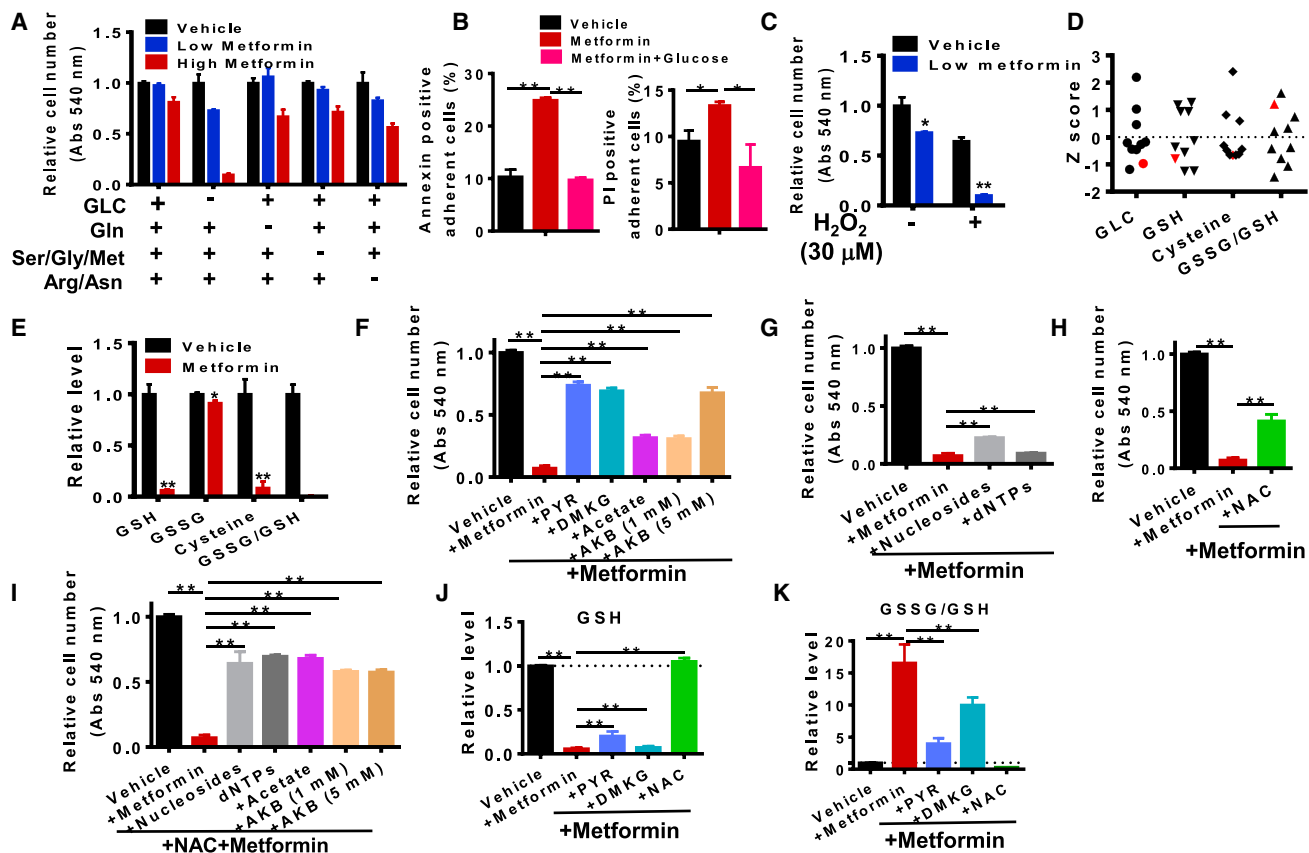
Figure 6. Metformin Response and Resistance Depends on the Availability of Specific Nutrients

(A) Response to metformin treatment in different medium conditions. Abs, absorbance (at 540 nm from MTT assay); GLC, glucose (11 mM); Gln, glutamine; Ser/Gly/Met, serine, glycine, and methionine; Arg/Asn, arginine and Asparagine; low metformin, 0.5 mM metformin; high metformin, 1.5 mM metformin.

(B) Metformin effect on cell proliferation in the presence of low glucose (1 mM) and/or hydrogen peroxide (H_2O_2, 30 μM).

(C) Annexin and PI positive populations of adherent cells after 40 hr of metformin treatment.

(D) Z score distribution of glucose (GLC) and redox metabolites (GSH, cysteine, and GSSG/GSH) in patients after metformin treatment. The long-term survivor is highlighted in red.

(E) Relative levels of redox metabolites in ovarian cancer cells with or without metformin treatment for 24 hr.

(F) Cell viability in the presence of metformin and precursors of the TCA cycle. PYR, pyruvate; DMKG, dimethyl α-ketoglutarate; acetate, sodium acetate; AKB, α-ketobutyrate.

(G) Rescue of metformin-induced loss of cell viability by nucleosides or deoxynucleotide triphosphates (dNTPs).

(H) Cell viability in defined conditions with or without N-acetylcysteine (NAC).

(I) Cell viability with the combination of noted nutrients and NAC.

(J) Relative level of GSH in different treatment conditions.

(K) Ratio of GSSG/GSH in different conditions.

*p < 0.05, **p < 0.01. Error bars obtained from SEM of n = 3 independent measurements.

in the tumor. Accordingly, critical aspects of mitochondrial metabolism were altered after metformin treatment, such as the levels of TCA intermediates, the accumulation of NADH, and the increase of reactive oxygen species (ROS). The accumulation of ROS could be attributed either to decreased glutathione (GSH) biosynthesis or electron leakage from electron transport chain, whose efficiency is inhibited by metformin. Aspartate biosynthesis was recently identified as the essential function of the respiratory chain (Birsoy et al., 2015; Cardaci et al., 2015; Sullivan et al., 2015). Although metformin inhibited nucleotide synthesis in several settings, aspartate, surprisingly, did not appear to be limiting in these conditions.

Because mitochondria function as a centralized hub in the metabolic network, we observed global metabolic reprogram-

ming in response to metformin treatment in human, mouse, and cell culture. Nevertheless, most of these metabolic alterations can be rationalized from a perturbation in mitochondrial metabolism, and rescue of metformin-induced cell death was achieved either by supplementing cells with mitochondrial substrates or combining nutrients that produce metabolites involved in downstream processes, such as nucleotides and antioxidants.

Metformin and Nutrient Limitations in the Mitochondria

Glucose concentrations were found to be less than 1 mM in tumors from OvCa patients. Consistently, cytotoxicity at physiologically meaningful doses of metformin is achieved when glucose availability is limited (Birsoy et al., 2014; Litchfield et al., 2015;
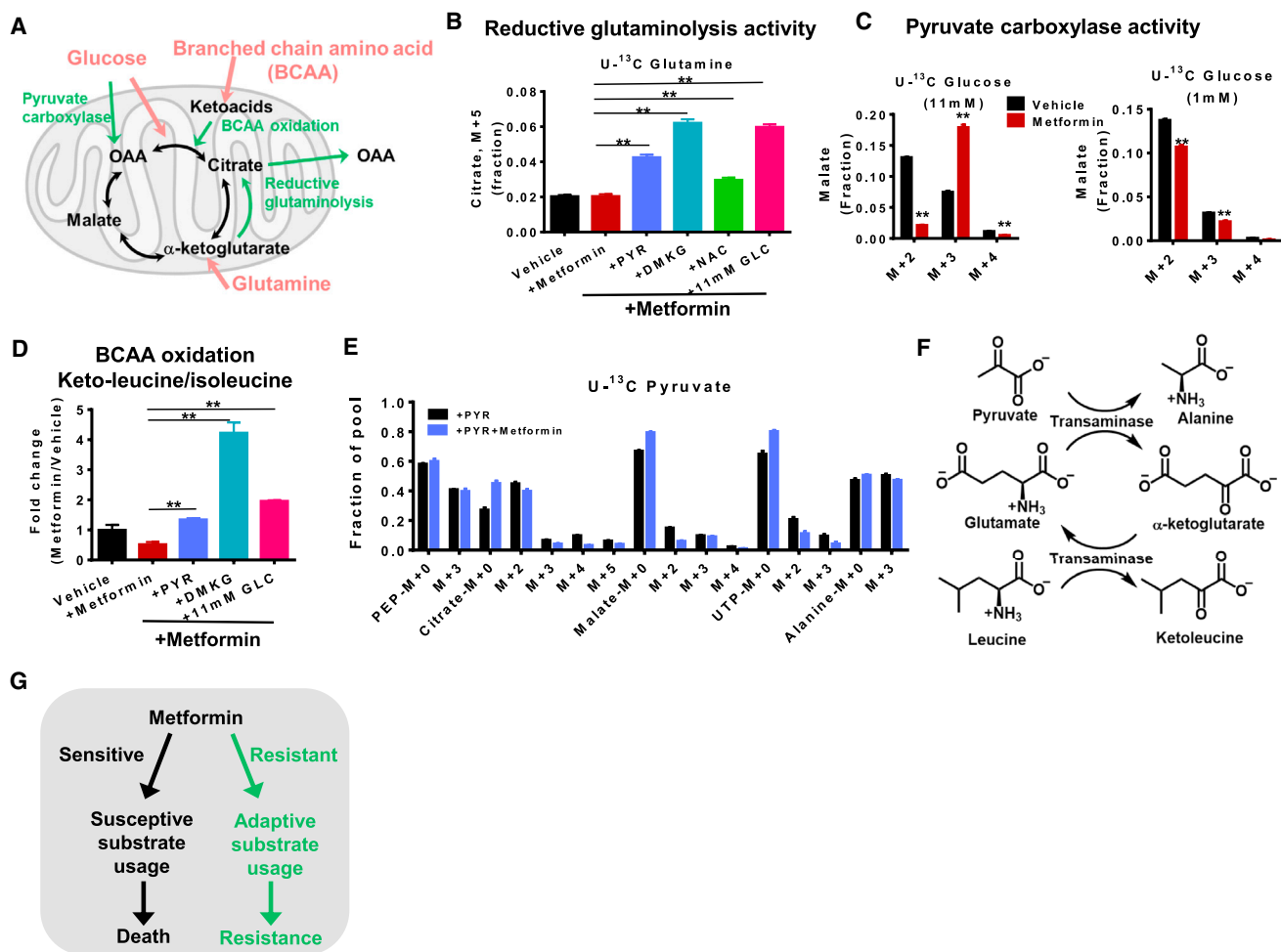
Figure 7. The Response to Metformin Depends on whether Substrate Utilization in the Mitochondria Is Flexible
(A) Schematic of substrate utilization. The adaptive pathways under mitochondrial stress are highlighted in green. OAA, oxaloacetate; keto acids, ketoleucine/ketoisoleucine.
(B) Reductive glutaminolysis activity as represented by the fraction of ^{13}C enriched citrate isotopologue (M+5) from cells treated with ^{13}C glutamine in different medium conditions.
(C) Pyruvate carboxylase activity as estimated by the fraction of malate (M+3) from cells treated with ^{13}C glucose in different medium conditions.
(D) Ketoleucine/ketoisoleucine levels in different media conditions, representing BCAA oxidation.
(E) Representative metabolite enrichment pattern from U-^{13}C pyruvate-treated cells.
(F) Scheme of coupled transamination reactions demonstrating stoichiometric α-ketoglutarate generation from alanine labeling.
(G) Model of resistant and sensitive response to metformin treatment. *p < 0.05, **p < 0.01. Error bars obtained from SEM of n = 3 independent measurements.

Wheaton et al., 2014). Interestingly, in conditions with sufficient nutrient availability, such as standard tissue culture conditions, cells readily resist metformin treatment by bringing other nutrients into the mitochondria to compensate for partially impaired ETC activity. Accordingly, metformin treatment enhanced pyruvate carboxylase activity and increased the reverse exchange flux in the TCA cycle, which resulted in increased production of malate, fumarate, and oxaloacetate and decreased flux along the TCA cycle. Such effects may also result in suppression of hepatic gluconeogenesis, which is thought to be a determinant of its mechanism of action in diabetes. Each of these features is thought to confer requirements for tumor growth in different contexts (Davidson et al., 2016; Hensley et al., 2016). However, in contrast to recent findings on biguanides and aspartate synthesis (Birsoy

et al., 2015; Cardaci et al., 2015; Sullivan et al., 2015), our data show that, under limiting conditions of nutrient availability, inhibition of the respiratory chain by metformin can actually cause secretion of aspartate as a waste product (Figure S4B). This finding exemplifies the heterogeneity of tumor metabolism and may extend to other cases where cells have certain respiratory chain defects, such as the case of succinate dehydrogenase mutations that increase dependence on pyruvate carboxylase (Cardaci et al., 2015). Thus, inhibition of the respiratory chain in proliferating cells does not always cause a defect in biosynthesis derived from aspartate metabolism.

We have reported that OvCa cells obtain fatty acids from adjacent adipocytes in the tumor microenvironment (Nieman et al., 2011). Here, we observed that catabolism of lipids by fatty acid

oxidation (FAO) could be used to fuel the TCA cycle in environments of limited glucose availability. However, when increased consumption of fatty acid was observed, cells were sensitive to metformin, likely due to the fact that FAO is much slower in fueling the TCA cycle relative to the rate of glucose or glutamine oxidation. Therefore, in glucose-limited conditions, adaptive pathways, such as FAO, that are upregulated and available in response to metformin are unable to fully compensate.

Finally, recent studies have suggested an enhanced dependency on mitochondrial metabolism during tumor dormancy or latency, a poorly characterized state of cancer cells that may underlie how tumors recur (Viale et al., 2014). Because nearly complete inhibition of the respiratory chain that can be achieved with compounds such as rotenone and cyanide is limited by toxicity, a speculative suggestion is that the safety profile of metformin may lend itself to a treatment for this cancer cell state of dormancy as a means to prevent recurrence.

Molecular Determinants of Metformin Action and a Long-Term Survivor

In addition to an overall signature pointing to alterations in mitochondrial metabolism across a set of human tumors, we further provide evidence, albeit an "n of 1," that a late-stage ovarian cancer patient taking metformin has an exceptionally long disease-free interval (long-term survivor) after surgical resection and exhibits numerous intratumoral features of what defined a response to metformin in both a mouse model of OvCa and cultured cells. It is understood that this long-term survivor provides only anecdotal evidence of a patient response to metformin; nevertheless, examples of defining a mechanistic basis for an exceptional patient response have led to numerous new and important insights (Grisham et al., 2015; Marx, 2015; Wagle et al., 2014). Typically, these responses are characterized by further validation of a predictive model for why a patient with a defined genetic lesion responded to a particular therapy. In this case, we show that a mechanistic basis of a long-term survivor can be understood through analysis of the specific metabolism occurring in the patient's tumor. Thus, knowledge of the metabolic profile of the tumor can be predictive of therapeutic response independent of cancer genetics.

Nevertheless, it is worth noting that there are several confounding factors in the patient study. The patients taking metformin had diabetes, the major clinical indication of its usage, and some patients were also taking other medications. Also, 2 other patients of the 20-patient total had not experienced recurrence at the time of this paper's submission; albeit, these patients were much closer to the time of their surgical resection. Nevertheless, we found signatures of mitochondrial inhibition in certain human tumors that we studied more deeply with model systems, and our conclusions were drawn from the integration of three independent systems (human, mouse, and cell culture).

Conclusions

The data presented to our knowledge provide the most comprehensive metabolomics analysis of metformin action in ovarian cancer to date. By integrating data from metabolic features remnant in human patient tumors with idealized responses in pre-clinical models, we were able to provide insight into the nature of metformin's effect on cancer. In doing so, we were also able to identify new aspects of metabolism that are controlled by mitochondria. With this deeper biochemical and systems-level understanding using a thorough metabolomics platform, we identified many of the pleiotropic features that determine an anti-cancer response to metformin. Hopefully these results will inform the design and patient selection for upcoming clinical investigations of this intriguing agent.

EXPERIMENTAL PROCEDURES

Reagents
A detailed list of reagents is provided in the Supplemental Information.

Animal
HeyA8 cells were injected intraperitoneally (Lengyel et al., 2014). Two weeks after injection, mice were treated with metformin (250 mg/kg/day) or placebo (PBS) administered intraperitoneally for an additional 4 weeks before mice were sacrificed. The mice were fed food and water ad libitum before sacrifice. Briefly, mice were anesthetized with isoflurane and euthanized with cervical dislocation. The time from sacrifice to flash freezing of the mouse tumors was approximately 2–4 min. The entire section of tumor was then stored at $-80°C$ before metabolomics analysis, and there was no additional processing performed. All animal procedures were approved by the Institutional Animal Care and Use Committee of the University of Chicago (#71951).

Patient Samples
Patient samples and clinical data were extracted from the biorepository and ongoing dataset of patients treated for OvCa at the University of Chicago. The last update on patient information was on May 1, 2016. As previously reported, the ovarian cancer dataset contains information on clinicopathologic parameters, use of metformin, and cancer outcomes (Romero et al., 2012). Recurrence of disease was defined using previously published clinical criteria (Therasse et al., 2000). Disease-free days were calculated from the date of diagnosis until the date of ovarian cancer recurrence or death. For patients without recurrence or death, the date of the last follow-up was utilized. Patients had been fasting overnight and until after surgery. Patient serum were collected after overnight starvation and before surgery. Patients were administered intravenous therapy (IV) with 278 mmol/L dextrose in normal saline before or during the surgery. Patients were under general anesthesia for a period of 30–90 min before surgery and stayed under anesthesia at the time of sample collection. The time from removal from the patient to flash freezing was less than 20 min. The entire section of human tumor was then stored at $-80°C$ freezer metabolomics analysis. There was no additional processing performed prior to metabolomics analysis. The institutional review board at the University of Chicago approved the study (#13372B and #13248A).

Cell Culture
The HeyA8 OvCa cell lines were provided by Dr. Gordon Mills. Cell lines were authenticated using CellCheck (IDEXX Bioresearch). HeyA8 cells were first cultured in a 10 cm dish with full growth medium containing RPMI 1640, 10% FBS, 100 U/mL penicillin, and 100 μg/mL streptomycin.

Cell Viability Assays
Cell viability was assessed using both tetrazolium-based MTT assay (Invitrogen) and cell counting (Moxi Z Mini Automated Cell Counter, ORFLO Technologies). The detailed procedure is described in the Supplemental Information.

Metabolite Extraction in Tumor and Serum
Both patient and mouse tumors were extracted as described previously (Liu et al., 2015) and also in the Supplemental Information. For absolute quantitation of metformin and glucose, $[^2H_6]$-metformin and ^{13}C-labeled standards were added to extraction solvent before metabolite extraction. More detailed information is included in the Supplemental Information.

Metabolite Extraction in Cell Culture

HeyA8 cells were seeded at a density of 150,000 cells per well in six-well plates. After overnight incubation in full growth medium, the old medium was removed, and cells were washed with 1 mL PBS before the addition of 2 mL of treatment medium. Glucose consumption and lactate secretion measurement are described in Supplemental Information. For intracellular metabolite analysis, after an incubation of 20 hr, metabolites were extracted as described in a previous study (Liu et al., 2014). Detailed information on ^{13}C tracing is provided in Supplemental Information.

Insulin Measurement

The concentration of insulin concentration in serum was measured using Ultra Sensitive Mouse Insulin ELISA Kit (Crystal Chem) according to the manufacturer's protocol. This insulin kit was kindly provided by Drs. Daniel Cooper and David Kirsch.

Apoptotic Cell Death

Phosphatidylserine on the external surface and propidium iodide uptake were measured using the Annexin V Alexa Fluor 488 and Propidium Iodide (PI) Dead Cell Apoptosis Kit (ThermoFisher Scientific) according to the manufacturer's recommendations. A detailed experimental procedure is described in the Supplemental Information.

Statistical Analysis and Bioinformatics

The LC-HRMS data analysis method is described in the Supplemental Information. Pathway analysis of metabolites using the Kyoto Encyclopedia of Genes and Genomes (KEGG) pathway database (http://www.genome.jp/kegg/) was carried out with Metaboanalyst software (http://www.metaboanalyst.ca). Principle component analysis (PCA) and statistical analysis were done using R programmer (https://www.r-project.org/). The metabolic network was constructed based on the Human Metabolome Database (HMDB) (http://www.hmdb.ca/) using open source software GAM (https://artyomovlab.wustl.edu/shiny/gam/). All data are represented as mean ± SEM. All p values were obtained from two-tailed Student's t test unless otherwise noted.

SUPPLEMENTAL INFORMATION

Supplemental Information includes Supplemental Experimental Procedures and six figures and can be found with this article online at http://dx.doi.org/10.1016/j.cmet.2016.09.005.

REFERENCES

Birsoy, K., Possemato, R., Lorbeer, F.K., Bayraktar, E.C., Thiru, P., Yucel, B., Wang, T., Chen, W.W., Clish, C.B., and Sabatini, D.M. (2014). Metabolic determinants of cancer cell sensitivity to glucose limitation and biguanides. Nature 508, 108–112.

Birsoy, K., Wang, T., Chen, W.W., Freinkman, E., Abu-Remaileh, M., and Sabatini, D.M. (2015). An essential role of the mitochondrial electron transport chain in cell proliferation is to enable aspartate synthesis. Cell 162, 540–551.

Bowtell, D.D., Böhm, S., Ahmed, A.A., Aspuria, P.J., Bast, R.C., Jr., Beral, V., Berek, J.S., Birrer, M.J., Blagden, S., Bookman, M.A., et al. (2015). Rethinking ovarian cancer II: reducing mortality from high-grade serous ovarian cancer. Nat. Rev. Cancer 15, 668–679.

Cabreiro, F., Au, C., Leung, K.Y., Vergara-Irigaray, N., Cochemé, H.M., Noori, T., Weinkove, D., Schuster, E., Greene, N.D., and Gems, D. (2013). Metformin retards aging in C. elegans by altering microbial folate and methionine metabolism. Cell 153, 228–239.

Camacho, L., Dasgupta, A., and Jiralerspong, S. (2015). Metformin in breast cancer—an evolving mystery. Breast Cancer Res. 17, 88.

Cardaci, S., Zheng, L., MacKay, G., van den Broek, N.J., MacKenzie, E.D., Nixon, C., Stevenson, D., Tumanov, S., Bulusu, V., Kamphorst, J.J., et al. (2015). Pyruvate carboxylation enables growth of SDH-deficient cells by supporting aspartate biosynthesis. Nat. Cell Biol. 17, 1317–1326.

Chandel, N.S., Avizonis, D., Reczek, C.R., Weinberg, S.E., Menz, S., Neuhaus, R., Christian, S., Haegebarth, A., Algire, C., and Pollak, M. (2016). Are metformin doses used in murine cancer models clinically relevant? Cell Metab. 23, 569–570.

Davidson, S.M., Papagiannakopoulos, T., Olenchock, B.A., Heyman, J.E., Keibler, M.A., Luengo, A., Bauer, M.R., Jha, A.K., O'Brien, J.P., Pierce, K.A., et al. (2016). Environment impacts the metabolic dependencies of Ras-driven non-small cell lung cancer. Cell Metab. 23, 517–528.

Decensi, A., Puntoni, M., Goodwin, P., Cazzaniga, M., Gennari, A., Bonanni, B., and Gandini, S. (2010). Metformin and cancer risk in diabetic patients: a systematic review and meta-analysis. Cancer Prev. Res. (Phila.) 3, 1451–1461.

Dowling, R.J., Lam, S., Bassi, C., Mouaaz, S., Aman, A., Kiyota, T., Al-Awar, R., Goodwin, P.J., and Stambolic, V. (2016). Metformin pharmacokinetics in mouse tumors: implications for human therapy. Cell Metab. 23, 567–568.

Evans, J.M., Donnelly, L.A., Emslie-Smith, A.M., Alessi, D.R., and Morris, A.D. (2005). Metformin and reduced risk of cancer in diabetic patients. BMJ 330, 1304–1305.

Ezewuiro, O., Grushko, T.A., Kocherginsky, M., Habis, M., Hurteau, J.A., Mills, K.A., Hunn, J., Olopade, O.I., Fleming, G.F., and Romero, I.L. (2016). Association of metformin use with outcomes in advanced endometrial cancer treated with chemotherapy. PLoS ONE 11, e0147145.

Febbraro, T., Lengyel, E., and Romero, I.L. (2014). Old drug, new trick: repurposing metformin for gynecologic cancers? Gynecol. Oncol. 135, 614–621.

Fendt, S.M., Bell, E.L., Keibler, M.A., Olenchock, B.A., Mayers, J.R., Wasylenko, T.M., Vokes, N.I., Guarente, L., Vander Heiden, M.G., and Stephanopoulos, G. (2013). Reductive glutamine metabolism is a function of the α-ketoglutarate to citrate ratio in cells. Nat. Commun. 4, 2236.

Forslund, K., Hildebrand, F., Nielsen, T., Falony, G., Le Chatelier, E., Sunagawa, S., Prifti, E., Vieira-Silva, S., Gudmundsdottir, V., Krogh Pedersen, H., et al.; MetaHIT consortium (2015). Disentangling type 2 diabetes and metformin treatment signatures in the human gut microbiota. Nature 528, 262–266.

Fullerton, M.D., Galic, S., Marcinko, K., Sikkema, S., Pulinilkunnil, T., Chen, Z.P., O'Neill, H.M., Ford, R.J., Palanivel, R., O'Brien, M., et al. (2013). Single phosphorylation sites in Acc1 and Acc2 regulate lipid homeostasis and the insulin-sensitizing effects of metformin. Nat. Med. 19, 1649–1654.

Grisham, R.N., Sylvester, B.E., Won, H., McDermott, G., DeLair, D., Ramirez, R., Yao, Z., Shen, R., Dao, F., Bogomolniy, F., et al. (2015). Extreme outlier analysis identifies occult mitogen-activated protein kinase pathway mutations in patients with low-grade serous ovarian cancer. J. Clin. Oncol. 33, 4099–4105.

Griss, T., Vincent, E.E., Egnatchik, R., Chen, J., Ma, E.H., Faubert, B., Viollet, B., DeBerardinis, R.J., and Jones, R.G. (2015). Metformin antagonizes cancer cell proliferation by suppressing mitochondrial-dependent biosynthesis. PLoS Biol. 13, e1002309.

Hensley, C.T., Faubert, B., Yuan, Q., Lev-Cohain, N., Jin, E., Kim, J., Jiang, L., Ko, B., Skelton, R., Loudat, L., et al. (2016). Metabolic heterogeneity in human lung tumors. Cell 164, 681–694.

Higurashi, T., Hosono, K., Takahashi, H., Komiya, Y., Umezawa, S., Sakai, E., Uchiyama, T., Taniguchi, L., Hata, Y., Uchiyama, S., et al. (2016). Metformin for chemoprevention of metachronous colorectal adenoma or polyps in post-polypectomy patients without diabetes: a multicentre double-blind, placebo-controlled, randomised phase 3 trial. Lancet Oncol. 17, 475–483.

Janzer, A., German, N.J., Gonzalez-Herrera, K.N., Asara, J.M., Haigis, M.C., and Struhl, K. (2014). Metformin and phenformin deplete tricarboxylic acid cycle and glycolytic intermediates during cell transformation and NTPs in cancer stem cells. Proc. Natl. Acad. Sci. USA 111, 10574–10579.

Jiralerspong, S., Palla, S.L., Giordano, S.H., Meric-Bernstam, F., Liedtke, C., Barnett, C.M., Hsu, L., Hung, M.C., Hortobagyi, G.N., and Gonzalez-Angulo, A.M. (2009). Metformin and pathologic complete responses to neoadjuvant chemotherapy in diabetic patients with breast cancer. J. Clin. Oncol. 27, 3297–3302.

Knowler, W.C., Barrett-Connor, E., Fowler, S.E., Hamman, R.F., Lachin, J.M., Walker, E.A., and Nathan, D.M.; Diabetes Prevention Program Research Group (2002). Reduction in the incidence of type 2 diabetes with lifestyle intervention or metformin. N. Engl. J. Med. 346, 393–403.

Koves, T.R., Ussher, J.R., Noland, R.C., Slentz, D., Mosedale, M., Ilkayeva, O., Bain, J., Stevens, R., Dyck, J.R., Newgard, C.B., et al. (2008). Mitochondrial overload and incomplete fatty acid oxidation contribute to skeletal muscle insulin resistance. Cell Metab. 7, 45–56.

Lengyel, E., Burdette, J.E., Kenny, H.A., Matei, D., Pilrose, J., Haluska, P., Nephew, K.P., Hales, D.B., and Stack, M.S. (2014). Epithelial ovarian cancer experimental models. Oncogene 33, 3619–3633.

Libby, G., Donnelly, L.A., Donnan, P.T., Alessi, D.R., Morris, A.D., and Evans, J.M. (2009). New users of metformin are at low risk of incident cancer: a cohort study among people with type 2 diabetes. Diabetes Care 32, 1620–1625.

Litchfield, L.M., Mukherjee, A., Eckert, M.A., Johnson, A., Mills, K.A., Pan, S., Shridhar, V., Lengyel, E., and Romero, I.L. (2015). Hyperglycemia-induced metabolic compensation inhibits metformin sensitivity in ovarian cancer. Oncotarget 6, 23548–23560.

Liu, X., Ser, Z., and Locasale, J.W. (2014). Development and quantitative evaluation of a high-resolution metabolomics technology. Anal. Chem. 86, 2175–2184.

Liu, X., Sadhukhan, S., Sun, S., Wagner, G.R., Hirschey, M.D., Qi, L., Lin, H., and Locasale, J.W. (2015). High-resolution metabolomics with Acyl-CoA profiling reveals widespread remodeling in response to diet. Mol. Cell. Proteomics 14, 1489–1500.

Madiraju, A.K., Erion, D.M., Rahimi, Y., Zhang, X.M., Braddock, D.T., Albright, R.A., Prigaro, B.J., Wood, J.L., Bhanot, S., MacDonald, M.J., et al. (2014). Metformin suppresses gluconeogenesis by inhibiting mitochondrial glycerophosphate dehydrogenase. Nature 510, 542–546.

Marx, V. (2015). Cancer: a most exceptional response. Nature 520, 389–393.

Miller, R.A., Chu, Q., Xie, J., Foretz, M., Viollet, B., and Birnbaum, M.J. (2013). Biguanides suppress hepatic glucagon signalling by decreasing production of cyclic AMP. Nature 494, 256–260.

Nieman, K.M., Kenny, H.A., Penicka, C.V., Ladanyi, A., Buell-Gutbrod, R., Zillhardt, M.R., Romero, I.L., Carey, M.S., Mills, G.B., Hotamisligil, G.S., et al. (2011). Adipocytes promote ovarian cancer metastasis and provide energy for rapid tumor growth. Nat. Med. 17, 1498–1503.

Pernicova, I., and Korbonits, M. (2014). Metformin—mode of action and clinical implications for diabetes and cancer. Nat. Rev. Endocrinol. 10, 143–156.

Romero, I.L., McCormick, A., McEwen, K.A., Park, S., Karrison, T., Yamada, S.D., Pannain, S., and Lengyel, E. (2012). Relationship of type II diabetes and metformin use to ovarian cancer progression, survival, and chemosensitivity. Obstet. Gynecol. 119, 61–67.

Shadel, G.S., and Horvath, T.L. (2015). Mitochondrial ROS signaling in organismal homeostasis. Cell 163, 560–569.

Shaw, R.J., Lamia, K.A., Vasquez, D., Koo, S.H., Bardeesy, N., Depinho, R.A., Montminy, M., and Cantley, L.C. (2005). The kinase LKB1 mediates glucose homeostasis in liver and therapeutic effects of metformin. Science 310, 1642–1646.

Sullivan, L.B., Gui, D.Y., Hosios, A.M., Bush, L.N., Freinkman, E., and Vander Heiden, M.G. (2015). Supporting aspartate biosynthesis is an essential function of respiration in proliferating cells. Cell 162, 552–563.

Therasse, P., Arbuck, S.G., Eisenhauer, E.A., Wanders, J., Kaplan, R.S., Rubinstein, L., Verweij, J., Van Glabbeke, M., van Oosterom, A.T., Christian, M.C., and Gwyther, S.G. (2000). New guidelines to evaluate the response to treatment in solid tumors. European Organization for Research and Treatment of Cancer, National Cancer Institute of the United States, National Cancer Institute of Canada. J. Natl. Cancer Inst. 92, 205–216.

Viale, A., Pettazzoni, P., Lyssiotis, C.A., Ying, H., Sánchez, N., Marchesini, M., Carugo, A., Green, T., Seth, S., Giuliani, V., et al. (2014). Oncogene ablation-resistant pancreatic cancer cells depend on mitochondrial function. Nature 514, 628–632.

Wagle, N., Grabiner, B.C., Van Allen, E.M., Hodis, E., Jacobus, S., Supko, J.G., Stewart, M., Choueiri, T.K., Gandhi, L., Cleary, J.M., et al. (2014). Activating mTOR mutations in a patient with an extraordinary response on a phase I trial of everolimus and pazopanib. Cancer Discov. 4, 546–553.

Weinberg, S.E., and Chandel, N.S. (2015). Targeting mitochondria metabolism for cancer therapy. Nat. Chem. Biol. 11, 9–15.

Wheaton, W.W., Weinberg, S.E., Hamanaka, R.B., Soberanes, S., Sullivan, L.B., Anso, E., Glasauer, A., Dufour, E., Mutlu, G.M., Budigner, G.S., and Chandel, N.S. (2014). Metformin inhibits mitochondrial complex I of cancer cells to reduce tumorigenesis. eLife 3, e02242.

Worth, A.J., Basu, S.S., Snyder, N.W., Mesaros, C., and Blair, I.A. (2014). Inhibition of neuronal cell mitochondrial complex I with rotenone increases lipid β-oxidation, supporting acetyl-coenzyme A levels. J. Biol. Chem. 289, 26895–26903.

Wright, J.L., and Stanford, J.L. (2009). Metformin use and prostate cancer in Caucasian men: results from a population-based case-control study. Cancer Causes Control 20, 1617–1622.

Zamboni, N., Saghatelian, A., and Patti, G.J. (2015). Defining the metabolome: size, flux, and regulation. Mol. Cell 58, 699–706.

Zhou, G., Myers, R., Li, Y., Chen, Y., Shen, X., Fenyk-Melody, J., Wu, M., Ventre, J., Doebber, T., Fujii, N., et al. (2001). Role of AMP-activated protein kinase in mechanism of metformin action. J. Clin. Invest. 108, 1167–1174.

Zong, W.X., Rabinowitz, J.D., and White, E. (2016). Mitochondria and cancer. Mol. Cell 61, 667–676.